International Journal of Computing and Digital Systems
ISSN (2210-142X)
Int. J. Com. Dig. Sys. #, No.# (Mon-20..)

Glaucoma Eyes Disease Identification: Using Vgg16 Model throughDeep Neural Network

Vaibhav C. Gandhi[1], Dr. Priyesh P. Gandhi[2]

[1] *Department of Computer Engineering, Gujarat Technological University, Ahmedabad, India*
[2]*Provost, Sigma University, Ahmedabad, India*
E-mail address: vaibhavgandhi2424@gmail.com, priyeshgandhi@gmail.com

Received ## Mon. 20##, Revised ## Mon. 20##, Accepted ## Mon. 20##, Published ## Mon. 20##

Abstract: Due to a rise in intraocular pressure, diabetes can potentially induce glaucoma, an optic nerve disease. Severe vision loss may result from the condition if it is not identified promptly. Artificial intelligence can be used to automate this procedure. Early illness diagnosis is therefore essential. The medical term "glaucoma" applies to several sensations rather than an actual disease. These symptoms are marked by elevated intraocular pressure (IOP) linked to an injury to the optic nerve and consequent loss or damage to retinal ganglion cells. However, elevated IOP is not the sole feature of glaucoma that requires or relates to changes in the visual field or damage to the optic nerve. Fundus image research has recently concentrated on the application of automated technology in Deep Learning (DL) based frameworks to extract manual features. Our approach involves utilizing unprocessed fundus images to train a hybrid ML and DL model how to aid experts in identifying indicators of glaucoma. A new framework from the Visual Geometry Group (VGG) is used to extract deep features. Popular traditional Machine Learning (ML) techniques for classification, involving Support Vector Machine (SVM), AdaBoost, Random Forest (RF), k Nearest Neighbour (kNN), and Multilayer Perceptron (MLP) have made use of deep features. Using the ACRIMA dataset of 705 imageries, the ML classifier and vgg16 models' performances were assessed. There are 80% training and 20% testing data in the dataset. Based on experimental data, the vgg16 emulate has the best success rate, with 94.6 sensitivity, 92.5% specificity, and 93.4% accuracy.

Keywords: Acrima, Deel Learning, Fundus Image, Glaucoma, ML Classifier, Vgg16

1. About Glaucoma

In the Hippocratic era (c. 400 BC), the Greek word glaōkvma (Glaucosis), Which basically meant that the greenish pupillary color in the eye, which differs greatly from the normal pupillary color, is what gave rise to the term "glaucoma." The clinical distinction between low visual acuity caused by glaucoma and cataracts was not established until the 17th century. Glaucoma was diagnosed as black cataract (Hindi: 'Kala Motia'), a phrase that is still widely used among rural Indians today, according to traditional Indian medicine. Two fundamental forms of glaucoma are associated with the traditional explanation for the greenish-blue tint in the pupillary region that was told in ancient times. The first type of glaucoma, known as acute primary angle closure glaucoma (PACG), is triggered by a blockage in the parietal region leading to a sudden surge in intraocular pressure (IOP). The manifestation of this condition includes intense headache, and severe eye discomfort, along with corneal clouding or haziness and redness [1,2].

The medical term "glaucoma" applies to several sensations rather than an actual disease. These symptoms are marked by elevated intraocular pressure (IOP) linked to injury to the optic nerve and consequent loss or damage to retinal ganglion cells. However, elevated IOP is not the sole feature of glaucoma that requires or relates to changes in the visual field or damage to the optic nerve [2,3].

Better quality of life and cost-effectiveness are made possible by early identification and timely treatment of glaucoma. Stressing the importance of regular eye examinations and screening initiatives is essential to promptly detecting glaucoma and preventing blindness. Understanding the severity of glaucoma and the critical role early identification has in preventing blinding consequences from the condition and minimizing the detrimental financial effects on society from preventable blindness [4].

E-mail:author's email

Collectively, the International Glaucoma Association and the International Glaucoma Patient Association established a worldwide effort to commemorate "World Glaucoma Day" on March 8th of each year, which coincides with International Glaucoma Week. In the same spirit, the United States Glaucoma Research Foundation has proclaimed January 2016 to be Glaucoma "Awareness Month" in the US. Despite such community-based efforts, developing nations, especially Southeast Asian rural and suburban areas have extremely minimal levels of glaucoma education and knowledge of the disease's lethality. Appropriate guidance through both traditional and digital outlets is vital to eliminating those barriers, raising the necessary public awareness, and expanding the message about health [4,5].

Worldwide, glaucoma is an increasing cause of irreversible eyesight. It is an eye illness imposed on by the destruction to the optic nerves. periodic examinations and medical care may delay visual loss if glaucoma is detected early. Blindness and loss of central vision can happen from the disease's irreversible, severe optic nerve damage if it is discovered too late. Early illness diagnosis is therefore essential. It is among the main reasons why eyesight loss is permanent. Recent years have seen the proposal of several methods for automatically identifying glaucoma concerning fundus imaging. Tragically, none of the treatments already in practice can completely remove significant levels of overlapping from fundus depicts applied for recognizing glaucoma, which might lower the accuracy as well as dependability of the conclusion [3,4,5].

Enhanced standard life expectancy along with monetary competitiveness are made possible by early detection and prompt therapy for glaucoma. Underscoring the need of regular vision checks and monitoring drives vitality and unquestionably assists in preventing the development of glaucoma and avoiding the risk of blindness. Being familiar with the serious nature of glaucoma and the vital significance that early identification has in averting blinding punishments from this disorder and avoiding the harmful financial consequences on communities from preventative eyesight.

An irreparable neuro-degenerative vision circumstance called glaucoma represents one of the main causes of blurry vision in across the globe. The World Health Organization (WHO) estimates that more than 65 million individuals worldwide are affected by this condition. Detecting and treating the condition early is essential for preventing any deterioration in vision, as it may not manifest noticeable symptoms. The main aspect of this silent eye illness is the loss of optic nerve fibers, which is brought on by amplified intraocular pressure (IOP) and/or inadequate body fluid circulation to the optic nerve. Yet because vision problems might exist without first elevating IOP, the measurement is unable to be sufficiently sensitive or particular to be utilized as a legitimate glaucoma medical diagnosis [4,5].

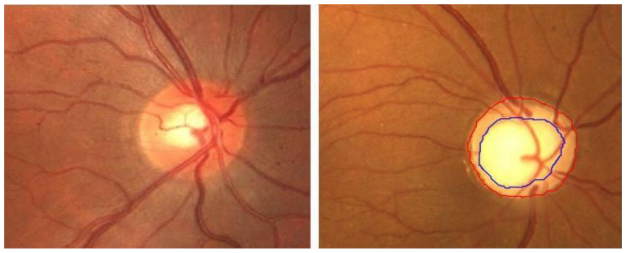

(a) (b)

Figure.1 Digital fundus visualizations containing an optic disc reduced (a) The main elements of an emitted sound disc with an optic and (b) Ophthalmic Eyesight loss disk.

The ganglion axon cells responsible for transmitting visual information to the optic nerve head are located in the optic disc. This area can be divided into two sections on a fundus image: the neuro-retinal rim, found at its periphery; and the bright central zone called an optic cup (as shown in Figure 1a on the left). Even though everyone has an optic disc (OD) and cup, glaucoma can be distinguished by an unusually large cup approximately the optic disc (see Right Side Figure 1b). Numerous algorithms have been developed to identify glaucoma in fundus images displaying the optic disc structure through segmentation of the optic disc and cup, owing to this circumstance. [3,4,5].

In certain make-believe investigations, the emphasis is placed solely on dividing up the optic cup and/or optic disc. However, in other cases, priority is given to determining the Cup/Disc ratio (CDR), which plays a critical role as an indicator of glaucoma. The CDR measures the vertical relationship between the eye's optic disc and vessels. Accurately measuring the CDR necessitates considerable effort in precisely dividing the optic disc and cup. Glaucoma, a chronic visual neuropathy, is primarily caused by increased vitreous pressure within the retina. It leads to a progressive reduction in the field of vision, potentially leading to irreversible blindness. Glaucoma, commonly known as the "silent steal of sight," may not exhibit initial indications of peripheral vision deterioration [3,4,5].

Early detection and prevention are crucial in halting visual loss progression as there is presently no cure for glaucoma. Investigative structures embrace visual field tests, optic nerve head examination, and intraocular pressure monitoring, but these assessments are susceptible to intra- and inter- observer oversights. Fundus photography is a valuable method for predicting glaucoma, but interpretation can be subjective. Computer-aided qualitative (CAD) systems address this by categorizing into three main types. The first calculates clinical indicators like CDR, ISNT rules, using segmented data. The second extracts data for glaucoma detection without classifying the image.

Many studies in glaucoma detection have used neither approach in the past, highlighting the evolving landscape of diagnostic methods [3,4,5].

2. LITERATURE SURVEY

In this section, a literature review is presented on DL based autonomous indicative techniques used for identifying glaucoma. The study methodologies, datasets, and experimental outcomes were taken under consideration when looking over the literature based on appearance. These investigations are categorized based on the types of visual findings that were used, encompassing fundus and Optical Coherence Tomography (OCT). Fully automated glaucoma diagnosis strategies based on retinal imaging primarily go through numerous processes encompassing feature extraction, segmentation, image quality improvement, and classification. Several of the problems with the literature on glaucoma detection have been deliberately evaluated and clarified within the portions of the article that follow.

As indicated by Satyabrata et al. [6], the presence of secularity reflections in retinal fundus imageries as a result of flash lighting might compromise their utility for detecting retinal diseases, although they remain an important diagnostic tool. This study suggests a pre-processing method for removing secularity from polluted fundus artwork. Four processes make up the method: feature extraction, segmentation using a modified U-Net CNN, extraction of specular reflections from the previously processed image, and SVM image classification. A high-intensity filter is used to ascertain the best method for obtaining diffuse and specular components. According to the model's testing results, PSNR and SSIM improved by a maximum of 37.97 dB during the pre- processing stage. The glaucoma experiment has been identified as successful, achieving an AUROC of 0.971 and demonstrating accuracy levels of 91.83%, sensitivity rates at 96.39%, and specificity readings of 95.37%.

According to Liu Li et al. (7), one of the main reasons behind visual impairment is glaucoma, which can be identified through fundus images in modern automated detection systems. None, however, can eliminate considerable redundancy, which could improve accuracy and dependability. If one wants to identify glaucoma, this article suggests using an attention-based CNN dubbed AG- CNN. The AG-CNN model utilizes a considerable glaucoma database of 11,760 fundus images categorized as either positive or negative based on attention. These images reveal localized problematic regions and are utilized for generating attention maps in the subnet. Results from experiments indicate that implementing this technique significantly enhances the identification of glaucoma beyond previous state-of-the-art methods.

Andres Diaz-Pinto et al. [8] This work introduces a novel method for automatically assessing fundus pictures for glaucoma, utilizing five ImageNet-trained models. The model is built on ACRIMA, the biggest public database for glaucoma diagnosis; it is well-known for its discriminative learning from raw pixel intensities. Extensive validation utilizing cross- validation techniques and cross-testing validation on all publicly accessible glaucoma-labelled databases supports the excellent specificity and sensitivity of the methodology. The goal of the project is to increase glaucoma diagnostic accuracy.

Abdelali Elmoufidi et al. [9] In ophthalmology, glaucoma is a developing issue as it can lead to blindness and avoid serious consequences. It is essential to discover these problems early to avoid them. This research describes a new image-based automated glaucoma diagnostic method. The Bi-dimensional Empirical Mode Decomposition (BEMD) technique is utilized by the framework to divide Regions of Interest (ROI) into smaller segments. These BEMD components are then used to derive distinctive features which are amalgamated as a set of features. Principal Component Analyses or PCAs assist in curtailing feature dimensionality. SVM is used as a foundation for the classifier's input parameters. ACRIMA and REFUGE, two open datasets, were used to train the models, while four more datasets were used for testing. The findings demonstrate the effectiveness and resilience of the suggested strategy and represent a significant advancement over previous research.

To identify glaucoma in color fundus imageries, Poonguzhali Elangovan et al. [10] provide a DL system based on a convolutional neural network (CNN). The goal of the 18-layer CNN is to categorize images of normal and glaucomatous fundus tissue. Four convolutional layers, two max-pooling layers, and one fully linked layer make up this structure. The network is tested on large-scale attention-based glaucoma datasets, including ORIGA, RIM-ONE2, ACRIMA, and DRISHTI-GS1. The design approach firmly opposes both Gaussian and salt-and-pepper noise, in contrast to other current methods.

A framework for DL using a CNN is proposed by Poonguzhali Elangovan et al. [10] to accurately identify glaucoma in color fundus images. The 18-layer CNN model includes four convolutional layers, two max-pooling layers and one fully connected layer. Its main objective is to discriminate amongst standard and glaucomatous eye images with high accuracy while resisting noise such as Gaussian or salt-and-pepper distortions that can hinder results. The study uses large-scale attention-based datasets of glaucoma cases including ORIGA, RIM-ONE2, ACRIMA and DRISHTI-GS1 to assure the efficacy of this new

approach compared against existing alternatives available today.

Serte S. et al. [12] Glaucoma is an advanced ocular condition causing blindness. Diagnosis involves perimetry, tonometry, and ophthalmoscopy. DL has been used for computer-aided detection. A comprehensive deep-learning model for recognizing glaucoma in fundus images is disclosed in this paper, exhibiting performance levels of 80% which are either comparable to or superior than those noted within previous works.

Asaoka R. et al. [13] conducted a study analyzing pre-perimetric glaucoma visual fields (VFs) from 53 eyes in 51 patients with open-angle glaucoma (OAG) and 108 healthy eyes in 87 participants. The researchers employed several ML techniques, including deep feed-forward neural network classifier to analyze the data's accuracy of discrimination measured using area under curve (AUC).

Chen X. et al. [14] Glaucoma is an advanced ocular condition causing blindness. Diagnosis involves perimetry, tonometry, and ophthalmoscopy. DL has been used for computer-aided detection. A comprehensive deep-learning model aimed at detecting glaucoma through analyzing fundus images is presented in this paper, achieving 80% accuracy which matches or outperforms existing literature.

Juneja M. et al. [15] This research presents the Classification of Glaucoma Network (CoG- NET), a deep network for glaucoma diagnosis. The network outperforms existing methods with 0.95 sensitivity, 0.99 specificity, and 93.5% accuracy. It focuses on the optical disc and cup in retinal fundus images, with an AUROC of 0.99. Using this strategy, glaucoma can be screened for at first.

TABLE 1 SUMMARY TABLE: MODERN ACCORDANCE ABOUT THE IDENTIFICATION OF GLAUCOMA DISEASES.

Work	*Method*	*Dataset*	*Performance*
[6]	Hybrid model U NetCNN	Mendeley data repository (2,206 anonymous retinal images)	Accuracy 91.83%
[7]	AB - CNN	Detailed attention-based glaucoma (LAG) database with 11,760 tagged fundus photos. Glaucoma .	Accuracy 96.22%
[8]	ImageNet-trained CNN architectures	Public databases (1707 images)	Accuracy 95%
[9]	VGG19	ACRIMA and REFUGE other open database	Accuracy 96
[10]	Xception	ACRIMA, Drishti-GS1, RIM-ONE	91.51% Accuracy 70.21% Accuracy 80% Accuracy 75.25% Accuracy 71.21% Accuracy70.82 % Accuracy
[11]	GoogLeNet	ACRIMA, HRF, Drishti-GS1, RIM-ONE sjchoi86-HRF	65% Accuracy 76% Accuracy 55% Accuracy 70% Accuracy 72% Accuracy
[12]	FNN		92.5% Accuracy
[13]	6 layer-CNN	ORIGA	0.831/0.887 Auc
[14]	CoG-NET	RIM-One, Drishti, REFUGE and ACRIMA	93.5% Accuracy

3. METHODOLOGY

The dataset is made up of 20% test data and 80% training data. Vgg16 was used to get deep features. Subsequently, the acquired characteristics were employed in various classification techniques, and the prediction procedure was executed. The effectiveness of the categorization techniques was evaluated through the use of performance indicators such as accuracy, specificity and sensitivity.

A. Dataset: ACRIMA

There exist several publicly accessible databases containing images labelled with glaucoma, which can be utilized for assessing glaucoma classification techniques. Consequently, the authors are delighted to present a novel publicly accessible glaucoma-labelled database named ACRIMA. The ACRIMA project curated this database of retinal images, gathered with consent from glaucoma and normal patients [9,10,11,14], in pursuit of developing automated classification algorithms.

Figure 2 presents a data set consisting of 705 images, including both glaucoma-positive (396) and glaucoma-negative (306) eye images. Among these color fundus images, the study utilized just 20%, or 142 for testing purposes. These were from the ACRIMA project (TIN2013-46751-R), a study to develop automated algorithms to assess retinal conditions that was funded by Spain's Ministerio de Economía y Competitividad. [19].

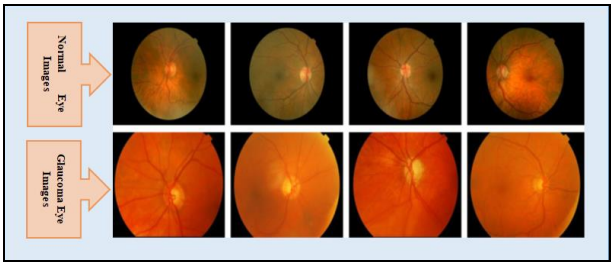

Figure 2. Publicly available databases have expanded with the addition of new examples. The recently released ACRIMA database offers a collection of both regular and Glaucoma fundus images.

In total, there were 705 images in the dataset. Among them, 396 had positive glaucoma classification and 306 exhibited negative results. For testing purposes, a subset of 142 color fundus images (accounting for one-fifth of the overall collection) was employed. Table 2 contains additional information about this dataset's characteristics and properties that can offer a more profound understanding of its features.

TABLE 2: DETAILS OF THE DATASET

Dataset Information	*Absence of Glaucoma*	*Presence of Glaucoma*
Training set	247	316
Test set	62	80
Total No. of Images	309	396

B. *Data Augmentation*

As a result, during pre-processing and testing, the pixel dimensions of the original picture collection were changed to 224x224 pixels for both the validation and training images to ensure compatibility with the model. Subsequently, grayscale conversion and cropping of the images were performed. Furthermore, to minimize overfitting due to limited data sizes in publicly available datasets [2,3,4,8], a zooming factor of 0.035 along with a rotation range of 0.025 was used for data augmentation; contrast- limited adaptive histogram equalization (CLAHE) was implemented post-cropping as well. To keep them looking similar to fundus photos, they weren't inverted. A 70-30 splitting ratio was used to split all datasets for testing and training [11,32].

C. *Preposed Methodology: Deep Neural Network Architecture for Learning*

Multiple layers and convolutional layers make up a Deep Neural Network, with the input layer receiving input. Figure 4 (VGG16 structure) depicts the VGG16 model's structure. As depicted in the picture, there are several layers- activation layer, flattening layer, maximum pool layer (max pool), and convolutional layer (conv). With the convolution filters included, the convolution layer generates the feature maps. Feature maps are fresh visuals that draw attention to the distinctive qualities of the CFIs. The image is filtered to achieve scaling. In the pooling layer, the image's size is decreased [5,6,7]. This is accomplished by setting a few neighboring pixels in the picture to their maximum value.

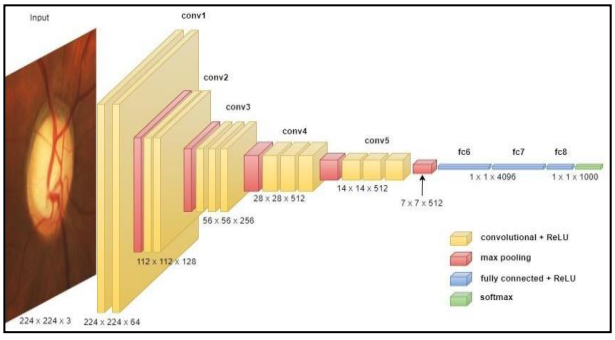

Figure 3. VGG16 Structure

The VGGNet-16 architecture (Figure 3 VGG16 Structure) has been constructed up of two separate components and comprises 16 layers. A stack of convolution layers has been used to process a picture to create an RGB image with dimensions of 224 x 224. Before being sent to the lowest two storage levels, a visualization (made up of 64 channels with 3 × 3 filter sizes) is sent to the top two layers. A convolution layer with 256 filters and two layers of 3 × 3 filters come after the max pool layer. First is the largest pool layer. Then, a max pool layer, two sets of three convolution layers, and one more set of three convolution layers have all been run several times. Instead of using 7 × 7 and 11 × 11, a 3 × 3 filter size is used in these convolution and max-pooling layers. After every convolution layer, Spatial characteristics are hidden in the image by applying one pixel of padding. [19].

The VGGNet-16 network design is demonstrated in Figure 3. The architecture comprises a series of convolution layers, succeeded by three completely associated layers before proceeding to another stack of convolutional ones. In the initial layer, they provide an input feature vector while maintaining a total channel number of 4,096 for the first two levels with maximum channels present in Layer One. Finally, we have Layer

Three, linked to the softmax layer and containing precisely one thousand channels.

TABLE 3: SPECIFICS OF THE LAYERS IN VGG16

Layer	Filter Size	PoolSize	Activation	Stride	Number of Parameters	Data Depth	Padding
Input	-	-	-	-	0	3	-
Conv1	5 * 5	-	RELU	1	36,928	32	Same
Max Pool	-	2*2	-	2	0	32	
Conv2	5 * 5	-	RELU	1	1,47,584	64	Same
Max Pool	-	2*2	-	2	0	64	
Conv3	5 * 5	-	RELU	1	5,90,080	128	Same
Max Pool	-	2*2	-	2	0	128	
Conv4	5 * 5	-	RELU	1	23,59,808	512	Same
Max Pool	-	2*2	-	2	0	512	
Conv5	5 * 5	-	RELU	1	23,59,808	1024	Same
Max Pool	-	2*2	-	2	0	1024	
Flatten	-	-	-	-	0	1024	-

D. Traditional: ML Classification Algorithm

A technique indicated in the current research for detecting glaucoma patients is shown in Figure 4As this image demonstrates pre-processing of the images from the retina had to be carried out in the first stage to obtain enhanced outcomes with a given data set.

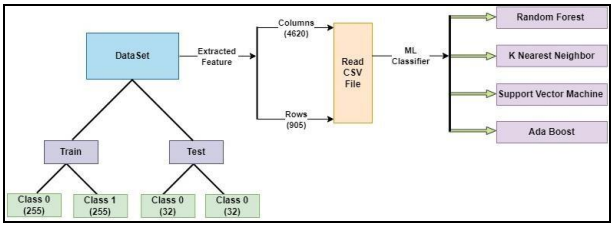

Figure 4. Traditional approach for identify Glaucoma using ML Classification

- SVM Classifier

Utilizing support vectors to determine the separating line between classes and optimizing margin, SVMs categorize input datasets into two precise classifications. To match a hyperplane and make the kernel SVM appropriate for nonlinear data, additional features can be included. SVM is an incredibly potent learning method that begins with a remarkably straightforward principle. The basis of SVM is rooted in the fundamentals of statistical learning and minimizing structural risk. While its theoretical approach involves separating examples belonging to distinct categories, it entails drawing two slender parallel boundary lines between the classes [2].

Data classification is achieved by utilizing a shared boundary line that runs parallel to, and maintains an equal distance from the two existing boundary lines. This concept led to the creation of very successful classifiers called SVMs. The SVM technique was employed to select the Hyperparameters through the use of grid search cross-validation. As a result, the RBF kernel and trade-off value of 0.01 were selected to carry out the classification procedure [17,27].

- Random Forest

Insufficient data leading to overfitting is a major concern when it comes to Decision Tree (DT) based models. Experts suggest resolving the problem by utilizing a model that comprises several decision trees, with each one employing distinct data sets. The Random Forest (RF) algorithm is a prime example of such a model, as it combines DT with various other methods. The decision trees that exhibit the highest levels of precision and autonomy are given preference [20]. The grid search cross-validation technique was utilized to ascertain the hyper-parameters of the RF algorithm. The classification process involved a maximum set of 1000 estimators and an auto value for the maximum feature parameter [16,17].

- K-nearest neighbors

Data is categorized using a fairly straightforward method called the K-nearest Neighbor (KNN), which measures how similar new data is to older data. By evaluating the separation between the data to be categorized and its neighbors, the algorithm establishes which label is most fitting for classification. This number of neighbors is used as a parameter by the algorithm to determine the contiguous period, and it is used to forecast the outcomes. The real number of neighbors is determined by comparing the data to the nearest neighbor percentage. By selecting the neighbors who are closest to each other based on the given number of neighbors, the KNN classification approach establishes that the unknown data is a member of the class with the largest total number of neighbors [17,20,27]. When determining the distance between data, two types of distance functions are commonly utilized: Manhattan and Euclidean. The hyperparameters of the KNN algorithm were determined through a meticulous grid search and cross-validation procedure. Equation 1 illustrates the computation of the Euclidean distance function,

which was employed to finalize the classification process by taking into account a total of 17 neighbors.

$$d(j,i) = \sqrt{\sum_{k=1}^{n}(x_{ik} - x_{jk})^2} \ldots\ldots(1)$$

- Adaptive boosting

Booster algorithms, also known as ML algorithms, are used in ensemble approaches. Ensemble method algorithms can produce a resilient knowledge process by coalescing many fragile learning algorithms. Because weak algorithms are usually easy to construct, they are frequently fast-derived versions of decision trees. Boosting techniques are similar to the ensemble approach for poor classifiers. By amalgamating several feeble classifiers, a formidable classifier can be created. However, throughout the process of development, a weight is allocated to every feeble classifier which grants improved accuracy in categorizing previously misclassified data. Consequently, the burdens of the learned models vary between samples. As more iterations are performed, the significance of unpredictable samples escalates, mandating that the model gives precedence to cases previously disregarded in earlier rounds [15, 17, 20, 22]. Adaptive boosting, or AdaBoost, is one of the highest eminent and established boosting algorithms. To determine the AdaBoost algorithm's hyper-parameters, grid search cross- validation was employed. As a result, the classification technique was performed with 1000 estimators and a learning rate of 0.1.

4. EXPERIMENTAL RESULTS

For this study, 309 fundus images of the normal class and 396 of the glaucoma-class were extracted from the ACRIMA dataset. A PC equipped with an AMD Ryzen 3500 4.1 GHz CPU, 16 GB RAM, and an NVIDIA graphics card (1x3060 and 1x1660 super) was used for the experimental investigations. The models were created using the Keras package and the Python programming language. In this study, the models' performance was assessed and the procedure was supported using the metrics of accuracy, sensitivity, and specificity. The confusion matrix is the source of these measurements, which are provided in Equations 2 through 5.

Values that are predicted to have glaucoma and do have it are referred to as true positives (TP). On the other hand, false negatives (FN) occur when values expected to be normal turn out to not be. False positives (FP), in contrast, happen when values projected with glaucoma don't end up having it. As for true negatives (TN), they refer specifically to numbers classified as non-glaucomatous but which upon further investigation were found abnormal after all.

$$Accuracy = \frac{TP+TN}{TP+TN+FP+FN} \ldots\ldots\ldots\ldots\ldots\ldots(2)$$

$$Precision = \frac{TP}{TP+FP} \ldots\ldots\ldots\ldots\ldots\ldots(3)$$

$$Sensitivity = \frac{TP}{TP+FN} \ldots\ldots\ldots\ldots(4)$$

$$Specificity = \frac{TN}{TN+FP} \ldots\ldots\ldots\ldots\ldots(5)$$

Generally, the ML classifier models underperform when it comes to recognizing glaucoma in imageries as compared to normal photos. Figure 5 presents a confusion matrix that was developed for evaluating individual model performance. Table 4 provides an overview of accuracy, sensitivity, and specificity values generated by each model. The study found that VGG16 outperforms the neural network model in terms of sensitivity, specificity, and accuracy performance indicators. The researchers also evaluated each VGG16's performance by analyzing their loss curves and accuracy models.

Table 4. The comparative result with ML Classifier and VGG16 models

Model	High-performance Parameters		
	Accuracy(%)	***Specificity(%)***	***Sensitivity(%)***
KNN classifier	73.1	38.5	92
Ada Boost Classifier	77.9	70	84
SVM Classifier	75	53.1	86.9
Radom forest Classifier	77.5	52	91.4
VGG16	93.4	92.5	94.6

- K- nearest Neighbor

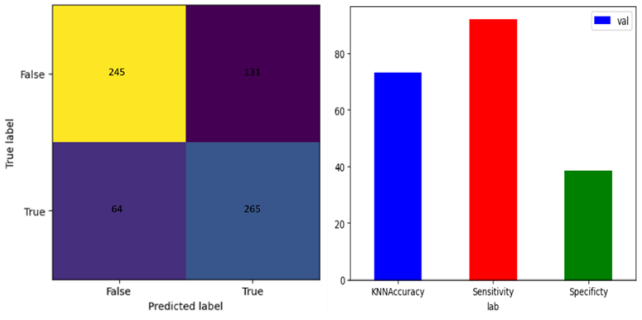

- Ada Boost

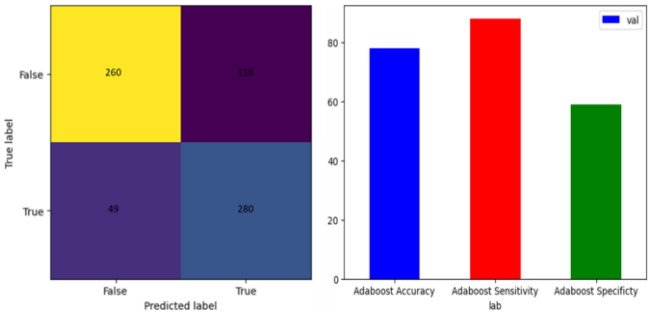

- SVM

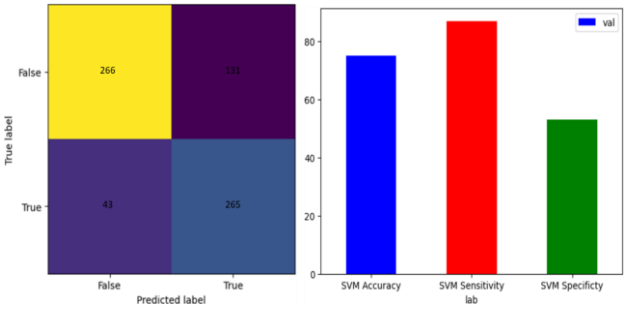

- Random Classifier

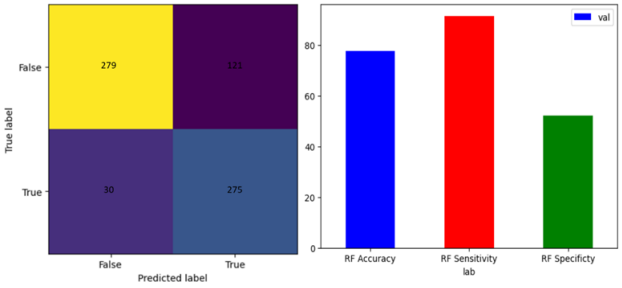

Figure 5. Confusion matrix obtained with ML Classifier various models

5. DISCUSSION

Below Figure 6(a) displays the Basic VGG16 confusion matrix and test image classification, and Figure 6(b) represents the accuracy and loss graphs, individually. The schemes illustrate the increase in accuracy rate and the reduction in damage proportion. The evidence presented illustrates that the model exhibits a rapid learning rate during both its training and learning processes. This is evidenced by the decreasing loss rates observed in each epoch of the working out procedure, accompanied by rising levels of accuracy as learning takes place through exposure to provided data sets. When each model's performance grew by very few units, the training was terminated. The suggested VGG16-based deep neural network model, however, received higher scores than the well-known other ML classifier models for the other success criteria.

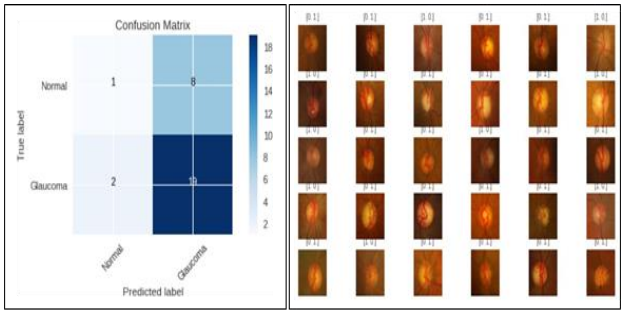

Figure. 6 (a) Confusion matrix obtained with Vgg16 (b) Test Image Classification using Vgg16

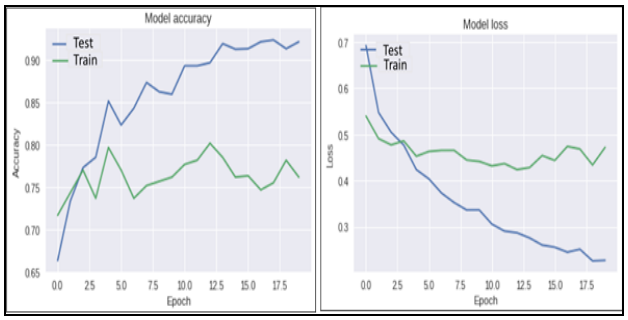

Figure 7. (a) The accuracy for the first training data collection over all epochs. (b) The training dataset's decline toward its epoch data set.

The suggested model outperformed previous investigations' techniques using various datasets from the existing literature in terms of outcomes [11,12,13,14]. Studies that include a large number of photographs in their dataset do well. While gathering a lot of data is frequently beneficial, doing so may be quite expensive. This instance demonstrated that having high-quality data, as opposed to a huge quantity, produces superior outcomes. The attention to detail must evolve from enormous data to quality data in many fields, including healthcare, where datasets featuring a portion of statistics are infrequent. The ultimate objective is to mitigate costs and boost performance in a model by enhancing the quality of the data during the data pre-preparation stage (noise reduction, for illustration).

Conclusion

The proposed study developed an ensemble model for timely detection of glaucoma. The model suggests using visual geometry group-16 to gather feature data from fundus photos in instruction to discriminate

amongst standard and glaucomatous imageries. The suggested ensemble creation method's performance is contrasted with three ML classifiers: SVM, KNN, Ada Boost, and Random Forest. The suggested method is evaluated using a variety of open data sets. The suggested algorithm performs better than the most advanced method available. The suggested collection model produces a precision rate of 93.4%, sensitivity of 94.6%, and specificity of 92.5% as applied to the ACRIMA dataset; testing was conducted on public datasets, demonstrating that the proposed design outperforms conventional computer-assisted diagnosis algorithms and vgg16 architecture models. The upcoming project aims at devising an entirely convolutional network with a wide-ranging experimental data set for segmenting optic cups and discs effectively in medical imaging analysis.

Using the ACRIMA data set, the recommended cooperative model produces an correctness of 93.4%, sensitivity of 94.6%, and specificity of 92.5%. Tests on the two public data sets establish that the suggested model performs better than the vgg16 architecture and conventional computer-aided indicative techniques. The creation of a completely convoluted network capable of segmenting optic discs and optic cups using a sizable experimental data set is investigated in the following suggested study.

ACKNOWLEDGMENT

The preferred spelling of the word "acknowledgment" in America is without an "e" after the "g". Avoid the stilted expression, "One of us (R. B. G.) thanks . . ." Instead, try "R. B. G. thanks". Put sponsor acknowledgments in the unnum-bered footnote on the first page.

REFERENCES

The template will number citations consecutively within brackets [1]. The sentence punctuation follows the bracket [2]. Refer simply to the reference number, as in [3]—do not use "Ref. [3]" or "reference [3]" except at the beginning of a sentence: "Reference [3] was the first . . ."

Number footnotes separately in superscripts. Place the actual footnote at the bottom of the column in which it was cited. Do not put footnotes in the reference list. Use letters for table footnotes.

Unless there are six authors or more give all authors' names; do not use "et al.". Papers that have not been published, even if they have been submitted for publication, should be cited as "unpublished" [4]. Papers that have been accepted for publication should be cited as "in press" [5]. Capitalize only the first word in a paper title, except for proper nouns and element symbols.

For papers published in translation journals, please give the English citation first, followed by the original foreign-language citation [6].

[1] Padmanayana and Dr.Anoop, "Binary classification of DR-diabetic retinopathy using CNN with fundus colour images," Mater. Today, vol. 58, pp. 212–216, 2022.
[2] R. E. Hacisoftaoglu, M. Karakaya, and A. B. Sallam, "Deep learning frameworks for diabetic retinopathy detection with smartphone-based retinal imaging systems," Pattern
Recognit. Lett., vol. 135, pp. 409–417, 2020.
[3] Z. Jin, F. Liu, W. Zhu, and W. Mu, "Weiping Wang ImageDC: Image Data Cleaning Framework Based on Deep Learning ,Yun Zhang," in IEEE International Conference on
Artificial Intelligence and Information Systems (ICAIIS), .
[4] F. Altaf and M. S. Syed, Naveed Akhtar And Naeem Khalid Janjua, "Going Deep in
Medical Image Analysis: Concepts, Methods, Challenges and Future Directions.
[5] Syna Sreng 1, Noppadol Maneerat 1, Kazuhiko Hamamoto 2 and Khin YadanarWin, Deep Learning for Optic Disc Segmentation and Glaucoma Diagnosis on," Retinal
Images in MDPI - Appl. Sci, vol. 2020, 2020.
[6] Z. L. Mayaluri and S. Lenka, "Hybrid glaucoma detection model based on reflection
components separation from retinal fundus images," EAI Endorsed Transactions on Pervasive Health and Technology, vol. 9, 2023.
[7] L. Li et al., "A large-scale database and a CNN model for attention-based glaucoma
detection," IEEE Trans. Med. Imaging, vol. 39, no. 2, pp. 413–424, 2020.
[8] A. Diaz-Pinto, S. Morales, V. Naranjo, T. Köhler, J. M. Mossi, and A. Navea, "CNNs for
automatic glaucoma assessment using fundus images: an extensive validation," Biomed. Eng. Online, vol. 18, no. 1, p. 29, 2019.
[9] P. Elangovan and M. K. Nath, "Glaucoma assessment from color fundus images using convolutional neural network," Int. J. Imaging Syst. Technol., vol. 31, no. 2, pp. 955–971,
2021.
[10] A. Elmoufidi, A. Skouta, S. Jai-Andaloussi, and O. Ouchetto, "CNN with multiple inputs
for automatic glaucoma assessment using fundus images," Int. J. Image Graph., vol. 23, no. 01, 2023.
[11] S. Serte and A. Serener, "A generalized deep learning model for glaucoma detection," in
2019 3rd International Symposium on Multidisciplinary Studies and Innovative Technologies (ISMSIT), 2019.
[12] R. Asaoka, H. Murata, A. Iwase, and M. Araie, "Detecting preperimetric glaucoma with standard automated perimetry using a deep learning classifier," Ophthalmology, vol. 123,
no. 9, pp. 1974–1980, 2016.
[13] X. Chen, Y. Xu, D. W. K. Wong, T. Y. Wong, and J. Liu, "Glaucoma detection based on deep convolutional neural network," in 2015 37th Annual International Conference of
the IEEE Engineering in Medicine and Biology Society (EMBC), 2015.
[14] M. Juneja, S. Thakur, A. Uniyal, A. Wani, N. Thakur, and P. Jindal, "Deep learning-
based classification network for glaucoma in retinal images," Comput. Electr. Eng., vol. 101, no. 108009, p. 108009, 2022.
[15] M. N. Bajwa et al., "Correction to: Two-stage framework for optic disc localization and
glaucoma classification in retinal fundus images using deep learning," BMC Med. Inform. Decis. Mak., vol. 19, no. 1, p. 153, 2019.
[16] Y. Chai, H. Liu, and J. Xu, "Glaucoma diagnosis based on both hidden features and domain knowledge through deep learning models," Knowl. Based Syst., vol. 161, pp.

147–156, 2018.
[17] N. Patil, P. N. Patil, and P. V. Rao, “Convolution neural network and deep-belief network (DBN) based automatic detection and diagnosis of Glaucoma,” Multimed. Tools Appl.,
2021.
[18] Y. Freund and R. E. Schapire, “A short introduction to boosting,” J-Japan Soc Artif Intell,
vol. 14, 1999.
[19] S. Saha, J. Vignarajan, and S. Frost, “A fast and fully automated system for glaucoma
detection using color fundus photographs,” Sci. Rep., vol. 13, no. 1, p. 18408, 2023.
[20] S. Gheisari et al., “A combined convolutional and recurrent neural network for enhanced
glaucoma detection,” Sci. Rep., vol. 11, no. 1, p. 1945, 2021.
[21] C. Oguz, T. Aydin, and M. Yaganoglu, “A CNN-based hybrid model to detect glaucoma
disease. Multimedia Tools and Applications,” Jul, vol. 17, pp. 1–9, 2023.
[22] V. C. Gandhi and P. P. Gandhi, “A Survey-Insights of ML and DL in Health Domain,”
in In2022 International Conference on Sustainable Computing and Data Communication Systems (ICSCDS), IEEE, 2022, pp. 239–246.

[23] J. Zilly, J. M. Buhmann, and D. Mahapatra, “Glaucoma detection using entropy sampling
and ensemble learning for automatic optic cup and disc segmentation,” Comput. Med. Imaging Graph., vol. 55, pp. 28–41, 2017.
[24] H. Raja, M. U. Akram, T. Hassan, A. Ramzan, A. Aziz, and H. Raja, “Glaucoma
detection using optical coherence tomography images: A systematic review of clinical and automated studies,” IETE J. Res., pp. 1–21, 2022.
[25] V. K. Shinoj, X. Hong, V. M. Murukeshan, M. Baskaran, and A. Tin, “Progress in anterior chamber angle imaging for glaucoma risk prediction-a review on clinical equipment, practice and research edical,” Eng Phys, vol. 38, no. 12, pp. 1383–1391,
2016.
[26] I. Tobore et al., “Deep Learning Intervention for Health Care Challenges: Some
Biomedical Domain Considerations in JMIR,”):e11966), vol. 7, 2019.
[27] Y. Weilu, C. Yiqiaoxing, and Y. Chen, “Changzheng Chen and YinShen “Applications of Artificial Intelligence in Ophthalmology: General Overview,” Artificial Intelligence in Ophthalmology: General Overview” in Hindawi Journal of Ophthalmology, vol. 2018, 2018.
[28] R. Miotto, F. Wang, S. Wang, X. Jiang, and J. T. Dudley, “Deep learning for healthcare: review, opportunities and challenges” Oxford University,” Briefings in Bioinformatics,
vol. 19, no. 6, pp. 1236–1246, 2017.
[29] W. G. H. A. W. Yu, A Survey of Deep Learning: Platforms, Applications and Emerging Research Trends in A Survey of Deep Learning: Platforms, Applications and Emerging
Research Trends, IEEEE acces. 2018.
[30] S. Joshi, B. Partibane, W. A. Hatamleh, H. Tarazi, C. S. Yadav, and D. Krah, “Glaucoma detection using image processing and supervised learning for classification,” J. Healthc.
Eng., vol. 2022, p. 2988262, 2022.
[31] Glaucoma Classification Dataset: ACRIMA,
https://www.kaggle.com/datasets/ayush02102001/glaucoma-classification-datasets
[32] Darji, M., Dave, J.A., Rathod, D.B. (2023). Review of Deep Learning: A New Era. In: Tuba, M., Akashe, S., Joshi, A. (eds) ICT Infrastructure and Computing. Lecture Notes in Networks and Systems, vol 520. Springer, Singapore. https://doi.org/10.1007/978- 981-19-5331-6_33

Vaibhav C. Gandhi is a Research Scholar in the Department of Computer Engineering at Gujarat Technological University. He received a bachelor's degree from Gujarat University and a master's degree from Gujarat Technological University. He is currently employed at CVM University as an assistant professor. He has more than 10 years of academic, software developer, research experience. He is a life member of various organizations, including ISTE, IAENG, and SDIWC. His areas of proficiency are Artificial Intelligence, Machine Learning, and Deep Learning. Furthermore, his research is on the ML/DL domain in the health-care industry, namely for the early detection of Glaucoma Disease.

Dr. Priyesh P. Gandhi, working as a Provost of Sigma University, Vadodara, Gujarat, India. He received his Ph.D. and M. Tech from Nirma University, Ahmedabad with specialization in VLSI Design. He has more than 17 years of academic and research experience. His area of interest is Analog and Mixed Signal VLSI Design, AI, ML and IOT.